Investigation of a Trailing Vortex Near Field by Stereoscopic Particle Image Velocimetry

M. Giuni* and R. B. Green †

University of Glasgow, Glasgow G12 8QQ, Scotland, UK

E. Benard‡

Institut Supérieur de l'Aéronautique et de l'Espace, 31055 Toulouse, FRANCE

High spatial resolution experiments in the near field of a trailing vortex using a SPIV technique have been carried out. A particular attention on the measurement technique is presented highlighting the importance of the laser pulses delay between the two frames in a double-frame/single-pulse method and of the images processing characteristics in the evaluation of velocity profiles and turbulence quantities. The number of samples needed for the statistical convergence of the mean flow and the turbulent quantities has also been found. A study on the vortex aperiodicity correction method has revealed how the instantaneous vector fields centering affects the velocity profiles across the vortex. The importance in the choice of the vortex quantity which is used for the vortex centre detection is presented.

Nomenclature

Δt	Laser pulse delay, μs
ΔX	Particle displacement vector, m
Γ	Overall circulation, m^2s^{-1}
AoA	Angle of attack, deg
b	Wing semi-span, m
c	Wing chord, m
d_I	Interrogation window size, m
d_L	Laser sheet thickness, mm
N	Number of averaged vector fields
r	Radial coordinate, m
Re	Reynolds number
u', v', w'	Velocity fluctuations RMS, m^2s^{-2}
U_∞	Freestream velocity, ms^{-1}
v_t	Swirl velocity, ms^{-1}
w	Axial velocity
x	Spanwise coordinate, m
y	Vertical upwards coordinate, m
z	Streamwise coordinate, m

I. Introduction

Wing tip vortices have been intensively studied over the last four decades. However a full understanding of the links between the numerous features that this flow exhibits is still lacking. The coexistence of cross boundary layer separations, high turbulence level, vorticity sheet rolling up, multiple vortices, diffusion, decay, collapse, instability of vortices are sources of major interest. In particular, a proven method to characterize and control the wake vortices is not available.[1]

Controlling wing tip vortices is of big importance with respect to the problems associated with their presence: noise generation in helicopters blades, hazard in following aircraft, separating distance and time between landing and take off in airports and cavitation in propeller blades. One of the main purposes of the research in wing tip vortices is therefore to reduce the effects of the vortex, by accelerating its decay.

The initial roll up of the vortex appears early over the wingtip, and the tip geometry plays a significant role in this process. While the flow cross-boundary layer separation in rounded wing tips always occurs on the suction surface, for flat tip the separation is fixed by the geometry since the flow has to turn more

*PhD Student, Department of Aerospace Engineering, AIAA Student Member.

†Senior Lecturer, Department of Aerospace Engineering.

‡Senior Lecturer, Department of Aerodynamics, Energetics and Propulsion.

abruptly over the sharp wing tip.[2] Furthermore, satellite vortices surrounding the main vortex have been detected in the near field,[3] and a strong secondary vortex has been observed more frequently in the high angle of attack cases.[4]

Theoretical studies on the vortex growing and evolution concentrate especially on the far field where the vortex is fully formed. A first analytical study describing the axial velocity inside a vortex was proposed by Batchelor.[5] The experimental fact that the flow is directed either towards the airplane (wake-like, as behind a nonlifting drag-producing body) or away from the wing (jet-like) was taken into account by a dissipation function. Spalart[6] explained the velocity excess as effect of the low pressure vortex core and the defect as the overcoming of the viscous effects proposing a circulation parameter $\Gamma/U_\infty b$ as the key parameter, with U_∞ is the freestream velocity and b is the wing semi-span. For example, Chow et al.[7] shows an excess axial velocity of $1.78U_\infty$ with a circulation parameter of 0.20 and, in contrast, Devenport et al.[8] reported a deficit of $0.85U_\infty$ corresponding to a circulation parameter of 0.028. Anderson et al.[9] have presented a wide range of tests for which the circulation parameter has been evaluated and experimental axial velocity measurements are reported showing a linear relation between this parameter and the axial velocity.

The complexity in the study and parameterization of the axial velocity arises because it is dependent on several factors: the exact wing geometry, the angle of attack, the Reynolds number, the downstream distance, the tangential velocity distribution, the wing boundary layer, details of the roll-up phase and the dissipation in the vortex.[10] Unlike the swirl velocity which is a hazard to other aircraft and is responsible for noise and vibration in helicopters, the effects of axial velocity are subtle. Though the axial velocity deficit/excess can be smaller in comparison to swirl velocity, its presence dictates to a large extent the stability and decay of the vortex. The axial flow is even known to play a significant role in vortex breakdown[11] and there is also concern about roof damage under the airport corridors resulting from the low-pressure core acting like a small tornado.[12]

The swirl or tangential velocity of a wing tip vortex has been widely studied focusing especially on the far field where the vortex structure is well defined. An analytical study by Phillips[13] led to the identification of three regions in the vortex based on the tangential velocity. Studies on the near field, and on the vortex formation and development have shown the sensible dependence from the tip geometry[2,14] and McAlister et al.[14] recorded a double inflection before the peak is reached that is suggested to be caused either by a secondary vortex which produced a second undulation also in the pressure distribution near the wing or by the crossing of the wing boundary layer as it wraps around the trailing vortex. This distortion completely disappears within one chord of distance from the trailing edge.

The problem of the wandering of the vortex has been well acknowledged although the reasons are a combination of freestream turbulence, wind tunnel walls effects, unsteadiness arising from the model or multiple vortices. Various procedures have been developed to correct vortex flow measurements for the resulting biasing effects. For one-point measurements, Devenport et al.[8] proposed a mathematical description of the wandering effects, the results of which provide methods for determining the amplitude of wandering and reversing those effects. For global measurements, such as PIV, the basic idea of all the methods is to collocate the centre of the tip vortex in each of the instantaneous velocity measurements frames before averaging.[15] The challenge therefore is in identifying a unique property of a tip vortex that can be used to define its center. Different methods have been used and studied and Ramasamy et al.[15] compared the uncorrected measures with five vortex centre detection methods: centroid of vorticity, peak axial velocity, helicity minimum, zero in-plane velocity and Q-criterion defined as the discriminant of a particular velocity gradient tensor. It was found that the method that best describes both the in-plane and out-of-plane quantities is the helicity aperiodicity correction because it includes all the velocity components in its calculation (cross product of out-of-plane vorticity and axial velocity). In their cases the vortex centre axial velocity was always detected as a deficit.

Because of the vortices are sensitive to even very small intrusive probes, combined with the presence of strong unsteadiness of the core flow, the small vortex core dimension and the core structure, Green[10] pointed out that the measuring technique to be adopted has to be global and non-intrusive or local, non-intrusive with conditional sampling. If the effects of the seeding are neglected, which is true in most cases (see Adrian et al.[16] or Raffel et al.[17] for particle dynamics), the PIV technique respects global and non-intrusive criteria. The amount of data obtained in a PIV and its processing require a comparable time and disk space resources with CFD simulations. A careful choice and validation of the key PIV parameters is therefore very important to know the accuracy and reliability of the tests.

II. Experimental Arrangement and Procedure

The experiments were conducted at the University of Glasgow in the low-speed "Argyll" wind tunnel, a closed-return facility with test section dimensions 2.65 m wide by 2.04 m high by 5.60 m. The model was a NACA 0015 wing with 0.42 m chord, 1.4 m span and rectangular wing tip (see Fig. 1(a)) allowing tests with small wall interference and blockage effects. The model was mounted on a plate outside the test section where height and angle of attack adjustments were set. The wing was positioned in the middle height of the test section with the tip along the centerline.

The reference system origin was on the wing tip trailing edge with x as spanwise coordinate, y vertically directed upwards and z coordinate along the freestream direction.

Two CCD cameras of 11 Mpixels were mounted on the sides of the test section independently from the wind tunnel (see Fig. 1(b)); 300 mm Nikon lenses were used and the f-number was 8. Angular stereoscopic system in Scheimpflug condition, as described by Zang and Prasad,[18] were adopted with angles between the camera and the object plane of around 35°. This value maintains low errors in the evaluation of both the in-plane and out-of-plane velocity component.[19] A double-frame/single-pulse method[20] was used so that for each time step two images were recorded for each camera corresponding to the two different laser pulses. The light source of the laser sheet was provided by a dual cavity Nd:YAG laser with 532 nm wavelength. A laser guiding arm was installed on a rail placed above the test section that allowed two-dimensional translations and three axes rotations of the laser. The laser sheet, of 3 mm of thickness, passed through a window on the top of the test section. The calibration of the cameras, the image acquisition, the laser control and the cross-correlation were accomplished by the LaVision software DaVis 7.2. A dual-plane calibration plate of 300 mm by 300 mm was used; the field of view of the cameras was of the same order. Every time the laser sheet was moved, a new adjustment of cameras (angles and separation) and a new calibration was performed.

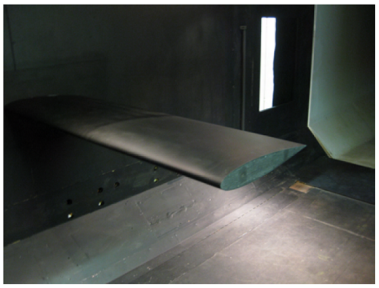

(a) Model and test chamber.

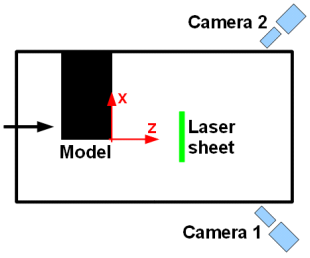

(b) Cameras and laser.

Figure 1. Experimental arrangement.

Several stereo cross-correlation processes of the image pairs were performed in order to test the result dependency on the images analysis method. The processed data were stored in an external hard disk of 1.5 TBytes.

The flow was seeded with olive oil particles by an Aerosol Generator PivPart40 serie installed at the end of the test section. The peak in the probability density function of the olive oil particles size distribution was at 1 μm that corresponds, following the procedure described by Adrian,[16] to a particle diameter between 1 and 2 pixels which is what suggested by Prasad et al.[21] to ensure a good quality in the correlation.

The wingtip vortex has been studied for Reynolds numbers of $1 \cdot 10^5$, $5 \cdot 10^5$ and $10 \cdot 10^5$ and angles of attack of the wing of 4°, 8°, 12° and 15° at planes perpendicular to the freestream at $z = 0.25$, 0.5, 1 and 2 chords from the trailing edge. Each test consisted in the acquisition of sets composed by 121 two images pairs at a constant frequency of 2 Hz.

A. Image processing

When choosing the image processing procedures for the cross-correlation of the images for stereo PIV, several factors have to be taken into account such as the the interrogation window size, the interrogation window overlap, the correlation procedure in terms of single or multi passes, the time needed for the operations and the memory required. Finding the compromise is therefore a crucial point.

For these experiments, a final interrogation window of 32 by 32 pixels gave the best compromise between smoothness of the results and spatial resolution (more then 40 points in the vortex core diameter). Smaller windows can not detect enough particles to give a statistically accurate result. A multi-pass procedure with a decreasing interrogation window is essential, especially for a correct evaluation of the out of plane velocity component.

There are two ways of increasing the spatial resolution: one is decreasing the interrogation window size and the other one is increasing the overlap. The first one encounters the limit of number of particles in each window, where the latter uses the same particle for several interrogation windows. Processing time and memory requirements were also an important factor in the choice of the images processing. Where iterative procedures do not really effect those parameters, interrogation window size and overlap are directly related to the number of vectors and so to the time and memory required.

An optimum compromise between all the factors has been found in a double step image processing on an interrogation window of 64 by 64 pixels with 25% of overlap followed by other two steps with interrogation window of 32 by 32 pixels with 50% of overlap leading to the calculation of 53300 vectors per frame and a velocity vectors spatial resolution around 1.2 mm corresponding to less then 0.3% of the chord.

III. Results and Discussions

A. Laser pulses delay

Time separation between successive laser pulses in PIV is a value that necessary needs to be taken into special consideration. In very simplistic way, the pulse separation should be short enough in order to do not lose too many particles in the interrogation window and long enough to allow the slowest particles to move a resolvable distance.

As described by Boillot and Prasad,[22] the restrictions change if the correlation is an auto-correlation (two pulses on the same frame) or a cross-correlation (two pulses on two different frames). In cross-correlations the delay time is not anymore dependent on the interrogation spot size d_I because they correlate an interrogation spot with another one which is displaced from the first spot by an amount equal to the local particle displacement vector ΔX (and also it can be deformed by the shear stress[23]) as evaluated in a previous step.

Keane and Adrian[20] showed that to achieve a valid detection probability of at least 90%, the image density (defined as the average number of particles per interrogation spot) must be greater than 15 with $\Delta X/d_I < 0.3$. This means that the pulses separation can also be seen as the time that the particles need to cover 30% of the interrogation spot size. In this way it is possible to link Δt with geometric quantities and a pre-knowledge of the flow (i.e. maximum in plane velocity):

$$\Delta t < \frac{0.3 d_I}{max|V|} \tag{1}$$

When the out of plane velocity component is high and the particle losses due to the cross velocity component, a second pulses separation relation can be written changing the interrogation spot dimension d_I with the laser sheet thickness d_L:

$$\Delta t < \frac{0.3 d_L}{max|V|} \tag{2}$$

A.1. Calculation of the time delay

Here are evaluated the time pulses separations from Eqs. (1) and (2) respectively considering in-plane displacements and out-of-plane displacements on a plane at $z/c = 0.5$, for an angle of attack of $AoA = 12°$ and $Re = 5 \cdot 10^5$ corresponding to a freestream velocity of $U_\infty = 17,26$ m/s.

For a Reynolds number of half a million a maximum in-plane velocity (tangential) of $0.9U_\infty$ and an excess vortex axial velocity of $1.6U_\infty$ are expected.

It is possible to apply Eq. (1) either on the object plane or on the image plane (on the chip). In the first case the interrogation window size will use the scale factor of 0.07145 mm/pixels where in the latter case the equation will use the pixel dimension on the chip of 0.009 mm/pixel and the magnification of the lens of 7.94. With an interrogation window size of 32 by 32 pixels, it obtains:

$$\begin{aligned} \Delta t < & \quad \frac{0.3 \cdot (32 \cdot 0.07145 \cdot 10^{-3})}{0.9 \cdot 17,26} = 44\,\mu\text{s} && \text{on the object plane} \\ < & \quad \frac{0.3 \cdot (32 \cdot 0.009 \cdot 10^{-3})}{(0.9 \cdot 17,26)/7.94} = 44\,\mu\text{s} && \text{on the image plane} \end{aligned}$$

The thickness of the laser sheet along the object plane was constant and equal to 3 mm, and the laser pulses separation from Eq. (2) can be then evaluated (on the object plane):

$$\Delta t < \frac{0.3 \cdot 0.003}{1.6 \cdot 17,26} = 33\,\mu\text{s}$$

The two separation times have resulted in a similar value that suggests good results for both the in-plane and out-of-plane velocity components. The in-plane time is affected by the interrogation window size chosen at the post processing stage where the out of plane time by the laser sheet thickness. Three time separations have then been compared: $\Delta t_1 = 15\,\mu$s; $\Delta t_2 = 35\,\mu$s; $\Delta t_3 = 55\,\mu$s.

One of the most common error affecting digital PIV is peak-locking,[17] a situation where the computed velocity fields have biased toward discrete values, resulting in the velocity vector maps to have block-like appearances. The velocity histograms for a peak-locked velocity field will then appear distorted and contain peaks. This situation occurs primarily because the small size of the seeding particles producing a sub-pixel particle image on the camera chip. In-plane and out-of-plane velocity histograms have been calculated for the three pulses delays, showing no peak-locking effects which indicates a well-conditioned experiment and analysis.

A.2. Results

Each one of the 121 vector fields was centered by the minimum helicity method and the average was then taken. Cuts every 30 degrees around the vortex centre, have been made and averaged tangential velocity profiles along these radius are plotted in Fig. 2. The red curves represent the average of the 12 profiles.

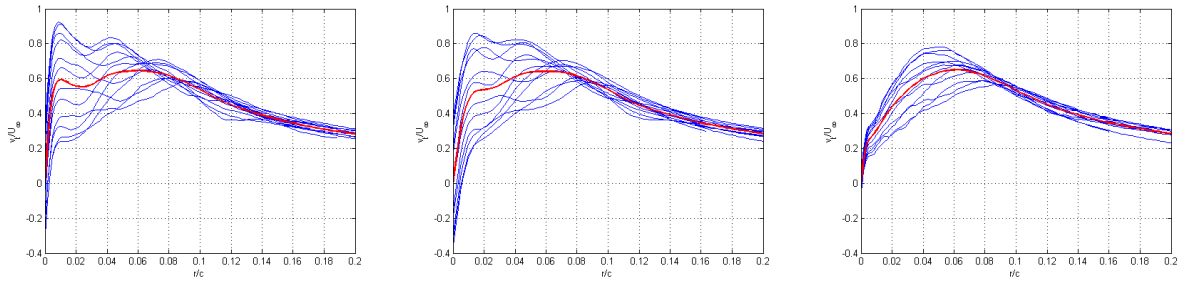

(a) $\Delta t = 15\,\mu$s. (b) $\Delta t = 35\,\mu$s. (c) $\Delta t = 55\,\mu$s.

Figure 2. Tangential velocity profiles as function of the laser pulses delay.

The topology of the tangential velocity profiles change radically with the laser pulses delay. The first 2 time separations show a high asymmetry of the vortex and a clear double peak also found by McAlister and Takahashi.[14] The long time delay does not show any second peak but only show the asymmetry found at this vortex stage. The maximum velocity observed also changes suggesting that with a Δt of 55 μs some faster particles are lost. It is also noted that the radius where the maximum averaged velocity is found (usually defined as the vortex core) remains in the same position at around 0.05 chords.

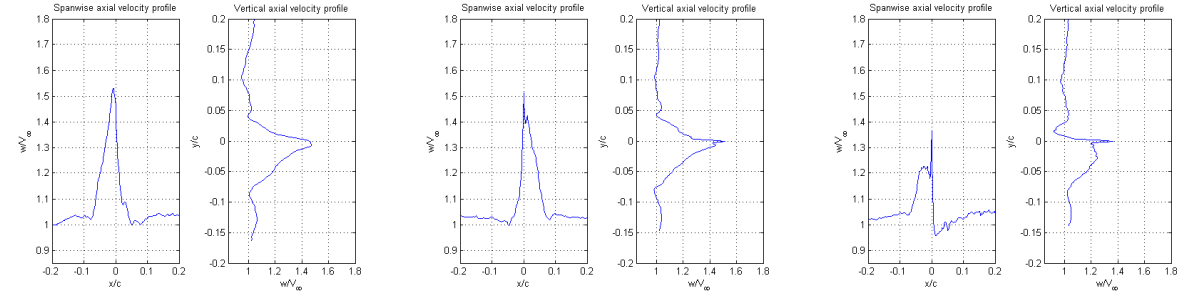

(a) $\Delta t = 15\,\mu$s. (b) $\Delta t = 35\,\mu$s. (c) $\Delta t = 55\,\mu$s.

Figure 3. Axial velocity profiles as function of the laser pulses delay.

Axial velocity has been evaluated for a horizontal and a vertical cut and shown in Fig. 3. A similarity between the profiles obtained with laser pulses separation of 15 μs and 35 μs is found also here. Also, the same conclusions of loss of particles can be made since the high pulse separation plot shows lower maximum axial velocity and a strong asymmetry that is not so marked for the other two laser pulses delays.

Average root mean squares of velocity fluctuations in Figs. 4, 5 and 6 show clearly their intensity growing with increasing the pulse separation time. Where between $\Delta t = 15\,\mu$s and 35 μs the distributions can be seen to be the same (i.e. the vorticose tail due to the vortex sheet rolling up around the main vortex), the $\Delta t = 55\,\mu$s tests show a more intense and different fluctuation level although the development along horizontal and vertical axis of u' and v' for all the cases is the same as observed by Ramasamy et al.[24]

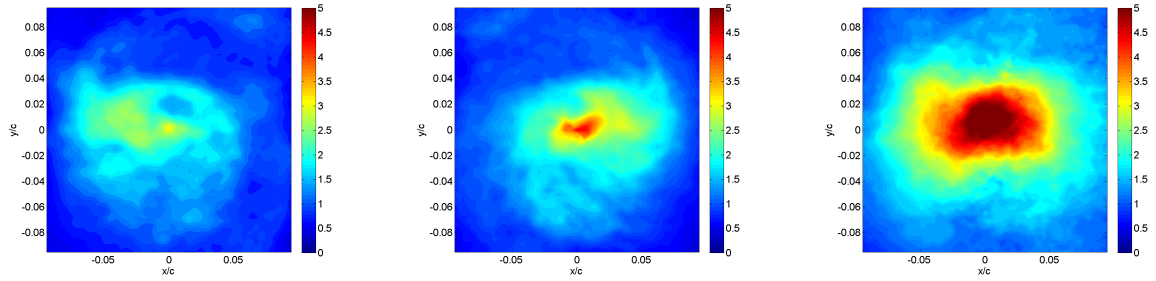

(a) $\Delta t = 15\,\mu$s. (b) $\Delta t = 35\,\mu$s. (c) $\Delta t = 55\,\mu$s.

Figure 4. Velocity fluctuations RMS as function of the laser pulses delay (u' component).

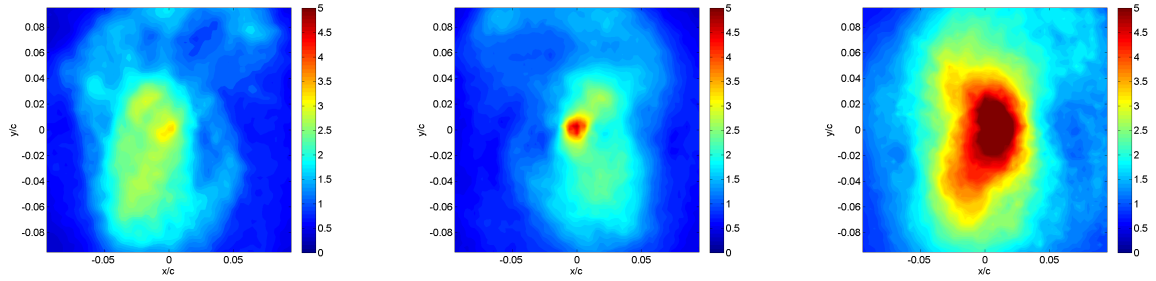

(a) $\Delta t = 15\,\mu$s. (b) $\Delta t = 35\,\mu$s. (c) $\Delta t = 55\,\mu$s.

Figure 5. Velocity fluctuations RMS as function of the laser pulses delay (v' component).

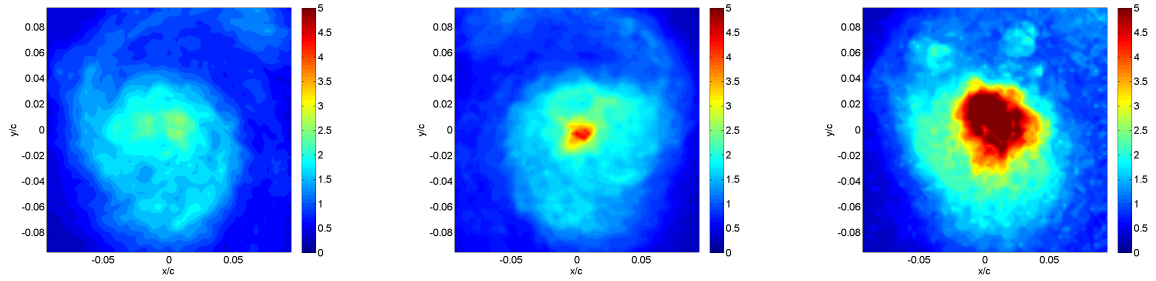

(a) $\Delta t = 15\,\mu$s. (b) $\Delta t = 35\,\mu$s. (c) $\Delta t = 55\,\mu$s.

Figure 6. Velocity fluctuations RMS as function of the laser pulses delay (w' component).

The results showed that a longer time introduces more turbulence and loses information in the region of high cross velocity (i.e. near the vortex centre) because the losses of particles moving across the laser plane reduce the accuracy of the displacement vector evaluation. In reverse a shorter time drastically reduces the turbulence without giving any additional information on velocity profiles in respect to the

middle pulse separation results. This behaviour can be attributed to the fact that a shorter time allows the particles to move by a smaller quantity which can be comparable to the uncertainty on the displacements (i.e. pixel). In other words, the minimum detectable in-plane velocity difference is the pixel size over pulses separation time so that decreasing Δt the minimum detectable velocity difference increases masking the turbulent fluctuations. For cross-plane velocity this is even more true because of geometric reasons: at camera angles as used, cross displacements are detected by the camera as a shorter vector than the same in-plane displacements. It is observed that the w' fluctuation for short time separation case is indeed very low compared to the other cases.

After these considerations, laser pulse time separation of 35μs has been used for the Reynolds number of half million, and similarly, 180μs for 100000 and 15μs for one million.

B. Averaging

Statistical convergence tests have been performed on velocity and turbulent fluctuations evaluations. Ramasamy et al.[24] found a minimum number of PIV images pairs required to achieve statistical convergence for the turbulent quantities equal to 250 for the first order characteristics, and about 750 samples for the second order characteristics.

The root mean square of the turbulence fluctuations and the second order turbulent quantities ($u'v'$, $u'w'$, $w'v'$) with shear strain (ϵ_{xy}), normal strain (ϵ_{zz}) and turbulent kinetic energy (TKE) are evaluated as function of the number of samples. Similar number of samples needed to achieve statistical convergence of what reported by Ramasamy et al.[24] are found.

For the turbulent fluctuations (see contours in Fig. 7 centered with helicity method), a minimum of 250 samples is required to reach the convergence where a minimum of 500 samples has been found to be required for the second order turbulent quantities . The shear strain, the normal strain and the TKE have been found to converges as the first order quantities.

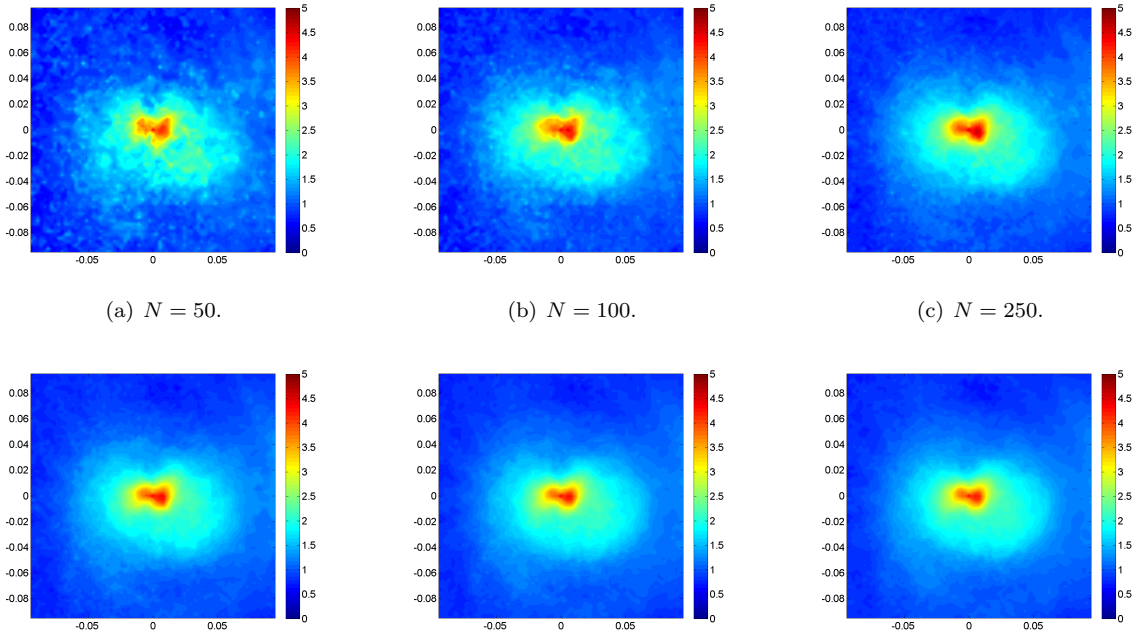

(a) $N = 50$. (b) $N = 100$. (c) $N = 250$.

(d) $N = 500$. (e) $N = 750$. (f) $N = 1000$.

Figure 7. Velocity fluctuations RMS for $z/c = 1$, $Re = 5 \cdot 10^5$, $AoA = 12°$ (v' component).

The tangential velocity profiles as function of the number of samples taken for the average are plotted in Fig. 8 where the helicity centering method was adopted. For a number of samples greater than 50 the statistical convergence is achieved.

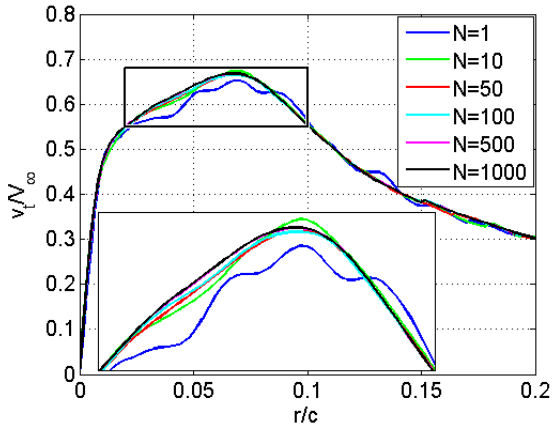

Figure 8. Averaged tangential velocity profiles as function of the number of samples for $z/c = 1$, $Re = 5 \cdot 10^5$, $AoA = 12°$.

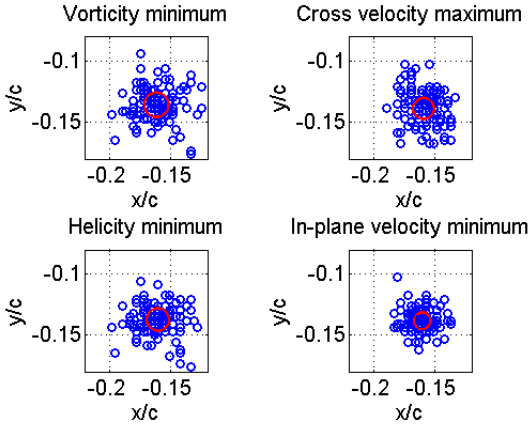

Figure 9. Vortex instantaneous centres evaluated with different centering methods for $z/c = 0.5$, $Re = 1 \cdot 10^5$, $AoA = 15°$.

C. Centering

Depending on which quantity and aspect of the vortex is of interest, the vortex centre detection method, which takes into account the aperiodicity of the meandering, can radically affect the results.

In order to visualize and quantify the wandering of the vortex, in Fig. 9 are plotted the instantaneous vortex centres of 121 samples as detected using four centering methods: vorticity minimum, cross velocity maximum, helicity minimum and zero in-plane velocity. A different scattering of the centres is observed with a standard deviation around two percent of the chord. Although the centre time histories are different when changing the detection method, the averaged positions are very similar.

The axial velocity profiles along eighteen diameters of the vortex are plotted in Fig. 10. Two cases are reported where for each one of them, three different centering methods have been applied: centering after the average and averaging after centering of each sample with the helicity and the axial velocity methods. The vorticity needed for the evaluation of the helicity has been calculated wit the circulation method as presented by Raffel.[17] Also plotted is the average of all the diameters in red.

A radical change in the sharpness and the symmetry of the profiles. As expected, the axial velocity centering method shows the maximum axial velocity peak in the vortex centre, with maximum velocity up to 20% higher. Furthermore, at low angles of attack, where the axial velocity vortex detection method shows a small excess in the centre, the other methods see a deficit.

It has been found by Giuni et al.[25] that for low angles of attack, the search of the axial velocity peak (either as excess of deficit with respect to the freestream velocity) is very critical because the vortex core appears as a region of low velocity with subregions of comparable excess and deficit velocity which rotates with the centre. This leads to a non-unique axial velocity peaks and a strong dependency on the searching technique. In contrast, at high angles of attack, the peak (velocity excess) is well defined and much more intense then the velocity deficit regions around it. The use of the axial velocity method is preferable when the study is focused on the axial velocity itself because it leads to higher and more defined peaks with the limit of questionable results at low angles of attack.

The tangential velocity along the 36 radii has also been plotted in Fig. 11 with the averaged profiles in red. The cases are the same as in Fig. 10 and a noticeable difference can be seen on the plane at $z/c = 0.25$, especially between the axial velocity method and the others, where at one chord the difference between the centering methods is small. This is an expected result since for a fully developed vortex all the methods lead to the identification of the same centre position.

The importance in clearly identifying and defining an aperiodicity correction method is highlighted and the particular features that are to be studied determine this choice. For this reason, comparisons with other experiments need to take into account and correlate the vortex centre detection methods that were adopted. This aspect has been found of extreme importance especially for the axial velocity.

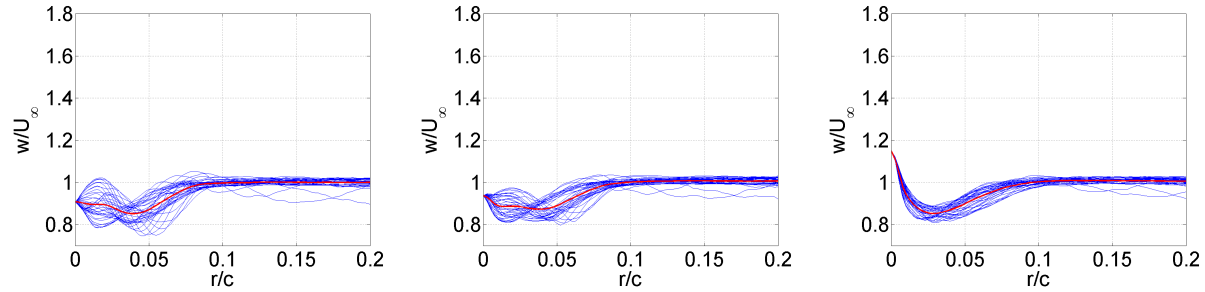

(a) $z/c = 0.25$, $Re = 1 \cdot 10^5$, $AoA = 4°$; no correction. (b) $z/c = 0.25$, $Re = 1 \cdot 10^5$, $AoA = 4°$; helicity method. (c) $z/c = 0.25$, $Re = 1 \cdot 10^5$, $AoA = 4°$; axial velocity method.

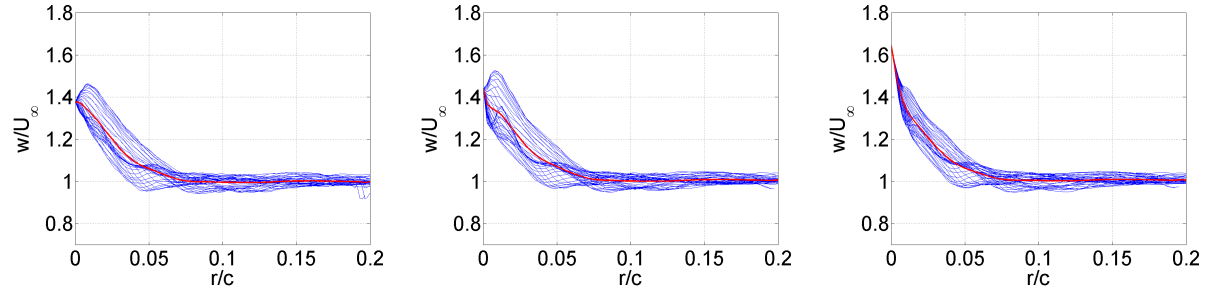

(d) $z/c = 1$, $Re = 10 \cdot 10^5$, $AoA = 12°$; no correction. (e) $z/c = 1$, $Re = 10 \cdot 10^5$, $AoA = 12°$; helicity method. (f) $z/c = 1$, $Re = 10 \cdot 10^5$, $AoA = 12°$; axial velocity method.

Figure 10. Axial velocity profiles.

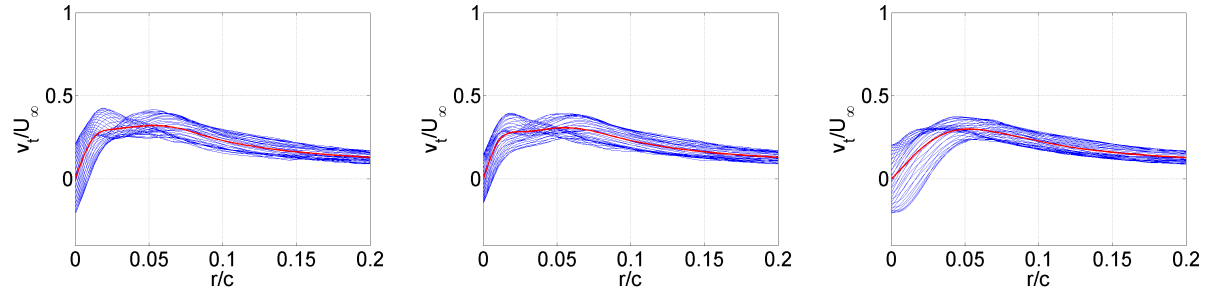

(a) $z/c = 0.25$, $Re = 1 \cdot 10^5$, $AoA = 4°$; no correction. (b) $z/c = 0.25$, $Re = 1 \cdot 10^5$, $AoA = 4°$; helicity method. (c) $z/c = 0.25$, $Re = 1 \cdot 10^5$, $AoA = 4°$; axial velocity method.

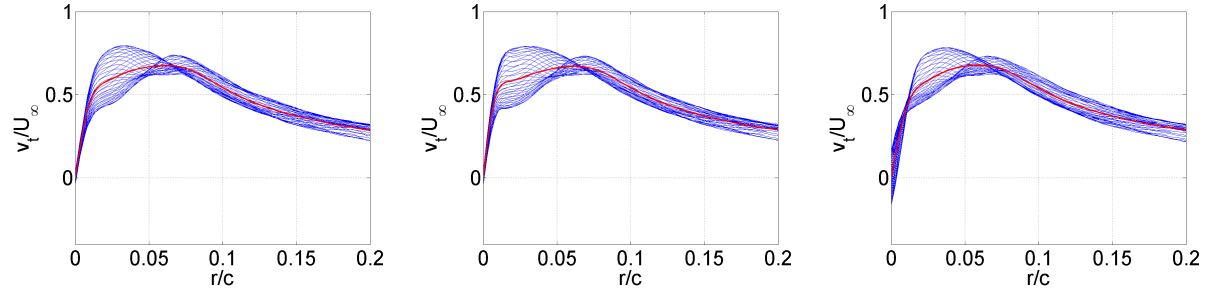

(d) $z/c = 1$, $Re = 10 \cdot 10^5$, $AoA = 12°$; no correction. (e) $z/c = 1$, $Re = 10 \cdot 10^5$, $AoA = 12°$; helicity method. (f) $z/c = 1$, $Re = 10 \cdot 10^5$, $AoA = 12°$; axial velocity method.

Figure 11. Tangential velocity profiles.

IV. Conclusion

High resolution experiments on the wing trailing vortex near field have been performed. An initial validation of the data highlighted the importance and strong dependency on the PIV laser pulse delay time

in detecting the vortex core structure and the turbulent quantities. In a particular way a second peak in the tangential velocity is lost for high pulses delays. A minimum number of 50 samples to achieve statistical convergence has been found for the velocity components. A number of 250 and 500 samples has been then found respectively for first and second order turbulent quantities. The sensitivity of the results to the aperiodicity correction method has been illustrated showing that the correct choice depends also on the feature that is going to be studied.

References

[1]Gerz, T., Holzapfel, G., and Darracq, D., "Aircraft Wake Vortices -A position Paper-," Wakenet position paper, April 2001.

[2]Duraisamy, K., *Studies in Tip Vortex Formation, Evolution and Control*, Ph.D. thesis, University of Maryland, College Park, 2005.

[3]Bailey, S. C. C., Tavoularis, S., and Lee, B. H. K., "Effects of Freestream Turbulence on Wing-Tip Vortex Formation and Near Field," *Journal of Aircraf*, Vol. 43, 2006, pp. 1282–1291.

[4]Zuhal, L. and Gharib, M., "Near Field Dynamics of Wing Tip Vortices," *31st AIAA Fluid Dynamics Conference & Exhibit*, AIAA, Anaheim, CA, 2001.

[5]Batchelor, G. K., "Axial Flow in Trailing Line Vortices," *Journal of Fluid Mechanics*, Vol. 20, No. 4, 1964, pp. 645–658.

[6]Spalart, P. R., "Airplane Trailing Vortices," *Annu. Rev. Fluid Mech.*, Vol. 30, 1998, pp. 107–138.

[7]Chow, J. S., Zilliac, G. G., and Bradshaw, P., "Mean and Turbulence Measurements in the Near Field of a Wingtip Vortex," *AIAA Journal*, Vol. 35, No. 10, 1997, pp. 1561–1567.

[8]Devenport, W. J., Rife, M. C., Lipias, S. I., and Follin, G. J., "The Structure and Development of a Wing-Tip Vortex," *Journal of Fluid Mechanics*, Vol. 312, 1996, pp. 67–106.

[9]Anderson, E. A. and Lawton, T. A., "Correlation Between Vortex Strength and Axial Velocity in a Trailing Vortex," *Journal of Aircraf*, Vol. 40, No. 4, 2003, pp. 699–704.

[10]Green, S. I., "Fluid vortices," *Fluid Mechanics and its Applications*, Kluwer Academic Publisher, 1995, pp. 427–470.

[11]Billant, P., Chomaz, J. M., and Huerre, P., "Experimental Study of Vortex Breakdown in Swirling Jets," *Journal of Fluid Mechanics*, Vol. 376, 1998, pp. 183–219.

[12]Lee, G. H., "Trailing Vortex Wakes," *Aeronautical Journal*, Vol. 79, 1975, pp. 377–388.

[13]Phillips, W. R. C., "The Turbulent Trailing Vortex During Roll-Up," *J. Fluid Mech.*, Vol. 105, 1981, pp. 451–467.

[14]McAlister, K. W. and Takahashi, R. K., "Wing Pressure and Trailing Vortex Measurements," Nasa technical report 3151, 1991.

[15]Ramasamy, M., Johnson, B., Huismann, T., and Leishman, J. G., "Digital Particle Image Velocimetry Measurements of Tip Vortex Characteristic Using an Improved Aperiodicity Correction," *Journal of the American Helicopter Society*, Vol. 54, No. 012004, 2009.

[16]Adrian, R. J., "Particle-Imaging Technique for Experimental Fluid Mechanics," *Annual Review Fluid Mechanics*, Vol. 23, 1991, pp. 261–304.

[17]M. Raffel, C. Willert, S. W. J. K., *Particle Image Velocimetry: a Practical Guide*, Springer, 2nd ed., 2007.

[18]Zang, W. and Prasad, K., "Performance Evaluation of a Scheimpflug Stereocamera for Particle Image Velocimetry," *Applied Optics*, Vol. 36, No. 33, 1997, pp. 8738–8744.

[19]Lawson, N. J. and Wu, J., "Three-Dimensional Particle Image Velocimetry: Error Analysis of Stereoscopic Techniques," *Meas. Sci. Technol.*, Vol. 8, 1997, pp. 894–900.

[20]Keane, R. D. and Adrian, R. J., "Theory of Cross-Correlation Analysis of PIV Images," *Applied Scientific Research*, Vol. 49, 1992, pp. 191–215.

[21]Prasad, A. K., Adrian, R. J., Landreth, C. C., and Offutt, P. W., "Effect of Resoluation on the Speed and Accuracy of Particle Image Velocimetry Interrogation," *Experiments in Fluids*, Vol. 13, 1992, pp. 105–116.

[22]Boillot, A. and Prasad, A. K., "Optimization Procedure for Pulse Separation in Cross-Correlation PIV," *Experiments in Fluids*, Vol. 21, 1996, pp. 87–93.

[23]Scarano, F., "Iterative Image Deformation Methods in PIV," *Meas. Sci. Technol.*, Vol. 13, 2002, pp. R1–R19.

[24]Ramasamy, M., Johnson, B., Huismann, T., and Leishman, J. G., "Procedures for Measuring the Turbulence Characteristics of Rotor Blade Tip Vortices," *Journal of the American Helicopter Society*, Vol. 54, No. 022006, 2009.

[25]Giuni, M., Benard, E., and Green, R. B., "Near Field Core Structure of Wing Tip Vortices," *Experimental Fluid Mechanics 2010*, EFM, Liberec, Czech Republic, 2010.